Nanofibrillation of deep eutectic solvent–treated paper and board cellulose pulps

Terhi Suopajärvi*, Juho Antti Sirviö, Henrikki Liimatainen

Fiber and Particle Engineering Unit, P.O. Box 4300, FI-90014 University of Oulu, Finland

Abstract

In this work, several cellulose board grades, including waste board, fluting, and waste milk container board, were pretreated with green choline chloride-urea deep eutectic solvent (DES) and nanofibrillated using a Masuko grinder. DES-treated bleached chemical birch pulp, NaOH-swollen waste board, and bleached chemical birch pulp were used as reference materials. The properties of the nanofibrils after disc grinding were compared with those obtained through microfluidization. Overall, the choline chloride-urea DES pretreatment significantly enhanced the nanofibrillation of the board pulps in both nanofibrillation methods—as compared with NaOH-treated pulps—and resulted in fine and long individual nanofibrils and some larger nanofibril bunches, as determined by field emission scanning electron microscopy and transmission electron microscopy. The nanofibril suspensions obtained from the DES pretreatment had a viscous, gel-like appearance with shear thinning behavior. The nanofibrils maintained their initial crystalline structure with a crystallinity index of 61% to 47%. Improved board handsheet properties also showed that DES-treated and Masuko-ground waste board and paper nanocellulose can potentially enhance the strength of the board. Consequently, the DES chemical pretreatment appears to be a promising route to obtain cellulose nanofibrils from waste board and paper.

Keywords: choline chloride, DES, fibrillation, nanocellulose, refining, waste board

1. Introduction

*Corresponding author. Tel. +358 294 482415. E-mail address: Terhi.suopajarvi@oulu.fi

Cellulose has recently gained significant attention as a green substituent for petroleum-based materials and chemicals and as a source for high-end products and applications. Nanoscale cellulose is especially regarded as a material with high potential due to its mechanical properties and chemical versatility as well as the diversity of its availability in raw materials. The definition of cellulose nanomaterials covers a wide range of nanoscale particles, including both stiff and elongated cellulose nanocrystals (CNC), with widths from 5 to 70 nm and lengths from 50 nm to several hundred nanometers and longer, and flexible and interconnected cellulose nanofibrils (CNF), with widths from 2 to 80 nm and lengths up to several micrometers (Azizi Samir, Alloin, & Dufresne, 2005a, 2005b; Lavoine, Desloges, Dufresne, & Bras, 2012).

Bleached chemical wood pulp has typically been used as a raw material for nanocellulose because most of the lignin, which hampers nanocellulose production, has already been removed from the wood matrix. However, virgin wood pulp fiber is also highly desirable for various other end uses, such as food packaging, and it has a relatively high value. Therefore, it would be beneficial to utilize secondary raw materials, such as waste paper and board, for nanocellulose production. Although these fiber materials may have shortened fiber lengths and decreased mechanical strength in the macroscale, they still maintain a high cellulose content (Danial et al., 2015; Josset et al., 2014).

Waste paper and board are highly abundant raw materials: within the EU, the recycling rate of paper and board was 81.1% in 2014 (Paper Packaging Coordination Group, 2016), and it has been at a high level in the United States as well—the recycling rate for old corrugated container board (OCC) was 91.2% in 2011 (Salam, Lucia, & Jameel, 2013). Therefore, waste paper and board are cheap raw materials that also contain large amounts of cellulose (Danial et al., 2015).

In addition to the cost of the raw materials, significant costs can be attributed to the nanocellulose production process. The mechanical separation of nanofibrils from fibers especially requires a high amount of energy because of the recalcitrant nature of cellulose, which is associated with a rigid and crystalline hydrogen bonded structure and which also makes cellulose insoluble in water and in most common organic solvents (Francisco, van den Bruinhorst, & Kroon, 2012; Zhang, Benoit, De Oliveira Vigier, Barrault, & Jérôme, 2012). This energy consumption can be reduced by up to 98% by using chemical pretreatments (Ankerfors, 2012), but many of these treatments are based on harmful and/or expensive chemicals, such as oxidation agents (Kuutti, Pajari, Rovio, Kokkonen, & Nuopponen, 2016; Liimatainen, Sirviö, Pajari, Hormi, & Niinimäki, 2013). Thus, green and inexpensive chemicals capable of loosening the recalcitrant nature of the cellulose structure are highly desired.

Recently, a new class of solvent called deep eutectic solvent (DES) has been investigated as a new, green media in biomass processing. A DES is easy to synthesize, is based on readily available bulk chemicals, and is biodegradable (Abbott, Boothby, Capper, Davies, & Rasheed, 2004). A DES system consists of two or more substances that form a eutectic mixture, which has a significantly lower melting point than that of any of its individual components, mainly due to the generation of intermolecular hydrogen bonds (Abbott et al., 2004; Sharma, Mukesh, Mondal, & Prasad, 2013; Q. Zhang, De Oliveira Vigier, Royer, & Jérôme, 2012). One of the most widespread chemicals used for the formation of a DES is choline chloride (Abbott et al., 2004; Q. Zhang, Benoit, et al., 2012). Choline chloride is a cheap, biodegradable, and non-toxic quaternary ammonium salt, which acts as a hydrogen bond acceptor (Abbott, Bell, Handa, & Stoddart, 2006; Abbott et al., 2004; Abbott, Capper, Davies, Rasheed, & Tambyrajah, 2003; Q. Zhang, Benoit, et al., 2012). Moreover, choline chloride is capable of forming a DES in combination with hydrogen bond donors, such as

urea, renewable carboxylic acids (*e.g.*, oxalic, citric, succinic, or amino acids), or renewable polyols (*e.g.*, glycerol or carbohydrates) (Dai, van Spronsen, Witkamp, Verpoorte, & Choi, 2013). Choline chloride–based DES solutions have been used previously to decrystallize microcrystalline cellulose (Q. Zhang, Benoit, et al., 2012), while a combination of choline chloride and urea has been used in the cationic functionalization of cotton cellulose (Abbott et al., 2006) and as a pretreatment for the nanofibrillation of wood cellulose (Sirviö, Visanko, & Liimatainen, 2015).

In this research, the production of cellulose nanofibrils from secondary cellulose fiber raw materials in the form of cellulose boards was investigated using a green choline chloride-urea–based DES pretreatment combined with disc grinding. Several board grades, including waste board (B), fluting (F), and waste milk container board (MCB), were used as raw materials. The characteristics of the nanofibrils obtained from the DES pretreated boards were compared with the nanofibrils obtained directly from the virgin bleached chemical birch pulp (BCP), NaOH-swollen waste board (NaOH-B), and bleached chemical birch pulp (NaOH-BCP). In addition, the properties of the nanofibrils obtained from disc grinding were compared with those obtained using a microfluidizer. Prepared nanocellulose samples were also tested as strength-enhancing additives in paperboard application.

2. Materials and Methods

Raw materials and chemicals

We obtained waste board (B) and milk container board (MCB) from the Finnish refuse collection, and both the fluting (F) and reference material, bleached chemical birch (*Betula verrucosa*) pulp (BCP), were obtained as dry sheets from Finnish pulp factories. The pulp (200 g abs) was pulped without chemicals using a Kenwood KM020 pulper (UK), with an operational principle similar to that of the Hobart pulper, for 10 minutes at a consistency of

1.5% and at approximately 45°C using a rotor speed of 2. The pulp was then washed and screened with a Somerville screen (Lorentzen & Wettre, Sweden). Approximately 38 wt.% of MCB pulp was screened away, as it is in plastic and aluminum foil.

The average (length-weighted) length and width of the fibers were determined with a Metso FiberLab image analyzer (Finland), and the charge of the pulp was analyzed via conductometric titration using a procedure described by Rattaz, Mishra, Chabot, & Daneault, (2011) and Katz, Beatson, & Scallan, (1984). The lignin content was determined using TAPPI-T 222 om-02 standard, and the extractive content was determined using SCAN-CM 49:03 standard. The determination of the hemicellulose content was performed with TAPPI-T 212 om-02 standard, ash content with ISO 1762 standard, and alkali solubility at 25°C with TAPPI-T 235 cm-00 standard. The fiber properties and chemical compositions of all cellulosic materials are shown in Figure 1.

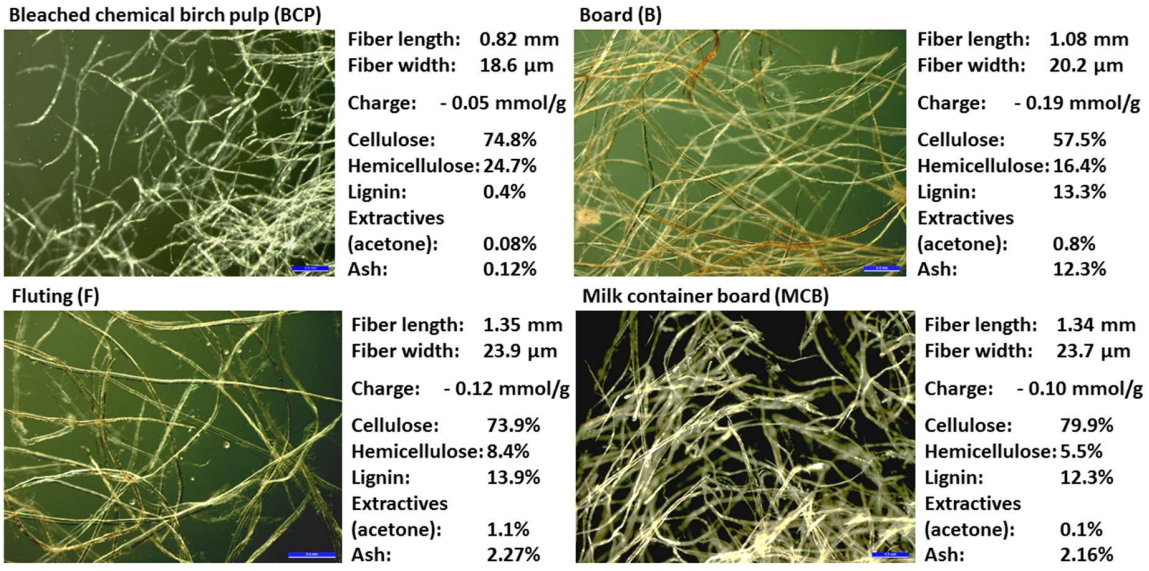

Figure 1. Fiber images via optical microscopy and the properties of the used pulp (scale bar 0.5 mm).

The choline chloride (98%) was obtained from Algry Quimica S.L. (Spain), urea (97%) from Borealis (Austria), and uranyl acetate (98%) from Polysciences (Germany).

Chemical pretreatments and nanofibrillation of cellulose materials

For the pulp pretreatment, the DES was produced by oven heating 1620 g of choline chloride and 1223 g of urea in a 5-liter beaker at 100°C until the mixture melted. Then, the mixture was placed into a water bath (100°C) under constant stirring for approximately five minutes to obtain a clear, colorless liquid. Next, 25 g (abs) of cellulose, at a consistency of ~30%, was added to the DES solution and mixed for two hours, after which the flask was removed from the water bath and 1000 ml of deionized water was added while mixing. The suspension was then washed with water in a Somerville screen until the washing water ran clear. Four batches of each pulp were treated with DES prior to nanofibrillation with a Masuko super masscolloider MKCA6-2J (Japan) grinder or a Microfluidics M-110EH-30 (USA) microfluidizer. As a reference material, 100 g (abs) of BCP and B were swollen with an NaOH solution overnight (pH ~12) at room temperature and washed with water in a Somerville screen prior to nanofibrillation with a Masuko grinder.

Before beginning nanofibrillation with the Masuko grinder, the stones of the grinder were first carefully brought within close contact, as observed by the low friction sound, and then the pretreated pulp slurry was poured into the grinder at a consistency of 1.5%. The pulp was passed twice through the grinder using a zero-grinding stone gap; then, the stones were adjusted to negative gap values to begin the actual nanofibrillation. Samples were taken after the first (-20 µm stone gap), third (additional passes with gaps of -40 µm and -50 µm), fifth (additional passes with gaps of -50 µm and -70 µm), eighth (additional passes with gaps of -70 µm, -80 µm, and -80 µm), and 10th (additional passes with gaps of -80 µm and -80 µm) passes.

DES-pretreated pulp (BCP, B, and F) was also nanofibrillated with the microfluidizer. At a consistency of 0.4%, each pulp was passed twice through 400 µm and 200 µm chambers at a pressure of 1500 bar (samples Fl-1), twice through 400 µm and 100 µm chambers at a

pressure of 2000 bar (samples Fl-2), and twice through 400 µm and 87 µm chambers at a pressure of 2000 bar (samples Fl-3).

Laboratory handsheets were prepared from board pulp with 4% of nanofibrillated pulps after 10 passes through the Masuko refiner and after the microfluidizer treatment in the presence of 0.08% retention aid and 4% of starch. Board sheets with 150 g/m^2 grammage were prepared in a laboratory sheet former (Lorentzen & Wettre, Sweden) according to the ISO 5269-1 standard method.

Characterization of the materials

Visualization

Each pulp was visualized during the nanofibrillation stages using a Leica MZ FLIII fluorescence stereomicroscope (Germany) and a Zeiss Ultra Plus field emission scanning electron microscope (FESEM) (Germany). As a pretreatment, the FESEM samples were filtered using a polycarbonate membrane with a pore size of 0.2 µm, followed by rapid freezing with liquid nitrogen and freeze-drying in a vacuum overnight. The dried samples were sputter-coated with platinum. An accelerating voltage of 5 kV and a working distance of 5 mm was used when imaging the samples. A Tecnai G2 Spirit transmission electron microscope (TEM) (The Netherlands) was used to observe the morphology of the end products after nanofibrillation. For the TEM observations, a small drop of the diluted nanofibril suspension was placed on a carbon-coated and poly-lysine-treated copper grid, and any excess sample was removed from the edge of the grid with filter paper. The samples were negatively stained with 2% (w/v) uranyl acetate, after which the samples were dried at room temperature. The TEM images were captured with a Quemesa CCD camera (Japan), using 100 kV as an accelerating voltage.

Rotational viscosity

Viscosity measurements of the cellulose nanofibril suspensions were performed with the Brookfield DV-II+ Pro EXTRA (USA) rotational viscometer. For these measurements, vane-shaped spindles (V-71, V-72, and V-73) were used at rotational speeds of 10, 20, 50, and 100 rpm. The consistency of the Masuko grinder–treated samples was 0.5%, and the consistency of the microfluidizer-treated samples was 0.3%; at a constant temperature (20°C), using a measurement time of 2–5 minutes for each rotational speed.

X-ray diffractometry

The crystallinity of the cellulose nanofibril samples was analyzed with wide-angle X-ray diffractometry (WAXD) using a Siemens D5000 diffractometer (USA); Cu Kα radiation (λ = 0.1542 nm) was used for the measurements. As a pretreatment, the freeze-dried samples were pressed into tablets at a thickness of 1 mm, and the scans were taken over a 2θ (Bragg angle) range from 5° to 50° at a scanning speed of 0.02°/s, using a step time of 1 s. The degree of crystallinity, or the crystallinity index (CrI), was calculated using a peak intensity of the main crystalline plane (200) diffraction (I_{200}) of 2θ at 22.8° and a peak intensity of 2θ at 18.0°, which is associated with the amorphous fraction of cellulose (I_{am}), according to Equation 1 (Segal, Creely, Martin, & Conrad, 1959):

$$CrI = \left(\frac{I_{200} - I_{am}}{I_{200}} \right) \times 100\% \qquad (1)$$

Mechanical handsheet properties

The board handsheets were conditioned before testing at 23°C in 50% relative humidity according to ISO 187 standard. The grammage and thickness of the board handsheets were measured according to ISO 536 and ISO 534 standards. Tensile strength of the board handsheets was measured according to ISO 1924-3 standard using 15 mm × 141 mm test strips.

3. Results and Discussion

The visual appearances of the DES- and NaOH-treated pulps after 10 passes through the Masuko grinder are shown in Figure 2. All of the DES-treated samples had gel-like, highly viscous appearances, but NaOH-swollen samples had a more watery composition at a consistency of ~1.5%. It is known that NaOH swells the fibers, loosening the structure of the cell wall, and thus may ease the nanofibrillation process. However, the NaOH-H_2O mixture does not dissolve the fibers with a high degree of polymerization (DP) at an ambient temperature but rather swells the fibers homogeneously without a balloon effect (S. Zhang, Wang, Li, & Yu, 2013). In DES treatments, used pulps were not added as oven dried; they actually consisted of about 70% water. However, Du, Zhao, Chen, Birbilis, & Yang (2016) recently stated that a small amount of water absorbed into the choline chloride-urea solution can even improve the electrolyte system in DES because water links to urea via strong hydrogen bonds, which promotes ionic dissociation by the generation of more free cationic choline ions (Du, Zhao, Chen, Birbilis, & Yang, 2016). During the DES treatment, the fibers rapidly formed a transparent, non-fibrous gel in the solvent, and after the addition of water, the fibers recovered their initial forms. Therefore, the fibers did not show any clearly visible changes in their structures after being washed with water.

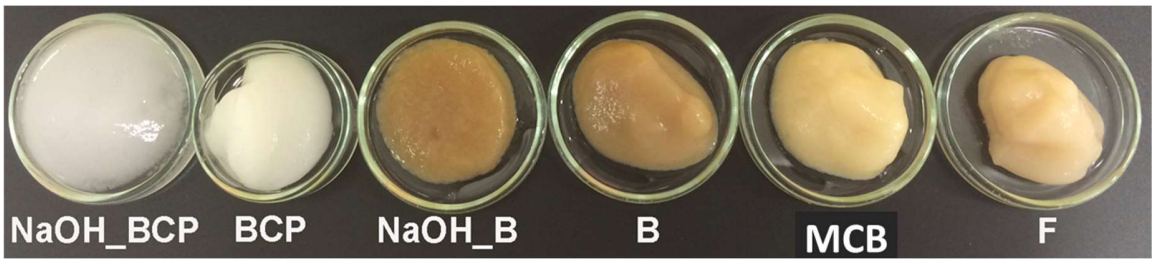

Figure 2. Visual appearances of the DES- (BCP, B, MCB, and F) and NaOH-treated pulps after the 10th pass through the Masuko grinder.

206 *Rotational viscosity*

207 Figure 3 shows the rotational viscosities of the DES/NaOH-treated and Masuko-ground
208 pulps after the eighth pass (Figure 3a) and after the 10th pass (Figure 3b) at a consistency
209 of 0.5%, and Figure 4 presents the rotational viscosities of the microfluidizer-treated pulps
210 after passing through the different chambers at a consistency of 0.3%. Low shear rate
211 viscosities correlate with the morphologies of cellulose particles (Besbes, Alila, & Boufi,
212 2011), and the higher the viscosity, the thinner and longer the nanofibrils are for a given
213 concentration (Lasseuguette, Roux, & Nishiyama, 2008). Long and thin nanofibrils are able
214 to form network structures in aqueous phases held together by numerous temporary
215 hydrogen bonds and Van der Waals interactions (Iotti, Gregersen, Moe, & Lenes, 2011).
216 This effect gives cellulose nanofibril suspensions thixotropic and shear thinning behavior
217 that is related to the high aspect ratio of the particles (Iotti et al., 2011; Mohtaschemi et al.,
218 2014).

219 After eight passes through the Masuko grinder (Figure 3a), the DES-treated reference BCP
220 had the highest viscosity, while the same pulp after the NaOH treatment had the lowest
221 viscosity, indicating the poor degree of nanofibrillation of the NaOH-treated pulp.
222 However, after the 10th pass through the Masuko grinder, the viscosity of the F pulp was
223 the highest of all the pulps (Figure 3b). Moreover, after the 10th pass, the BCP and B pulp
224 had similar viscosities, while both NaOH-treated pulps clearly had the lowest viscosities of
225 all the pulps. The MCB pulp had the lowest viscosity of the DES-treated pulps, indicating
226 that this pulp likely contained larger nanofibril bunches or aggregates instead of individual
227 fibrils. The visual observations also showed that the MCB sample had the longest
228 nanofibrils.

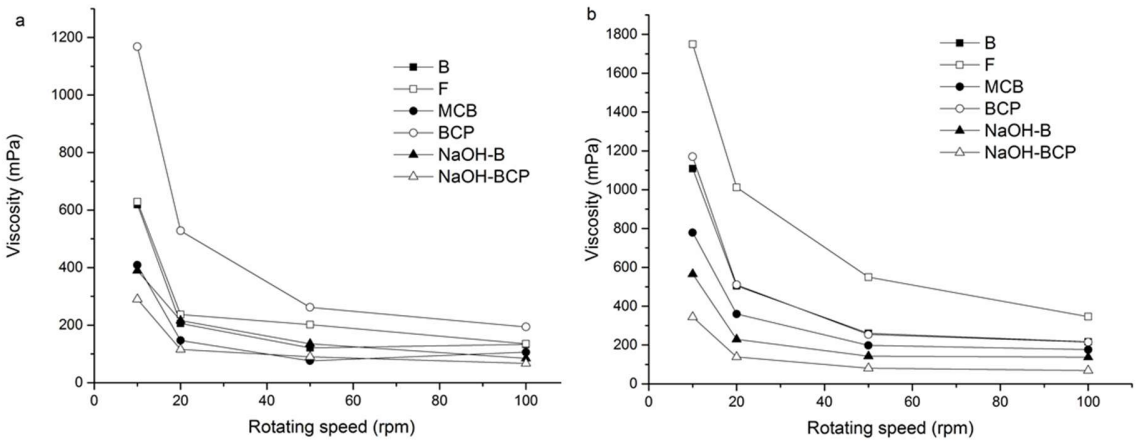

229 **Figure 3.** Rotational viscosities of the DES- (BCP, B, MCB, and F) and NaOH-treated and
230 Masuko-ground pulps a) after the eighth pass and b) after the 10th pass at a consistency of
231 0.5%.

232 For comparison, selected DES-treated pulps were also nanofibrillated using a
233 microfluidizer to investigate the role of the disintegration method in nanofibrillation
234 behavior. The microfluidized DES-treated pulps showed results similar to those of the
235 Masuko-ground pulps in their viscosity behavior (Figure 4). However, the viscosity of the
236 BCP was already the highest at the beginning of the nanofibrillation (Figure 4a), but after
237 passing through the next set of chambers (400 µm and 100 µm), the F pulp had the highest
238 viscosity, similar to that of the Masuko-ground pulp (Fig. 4b and c).

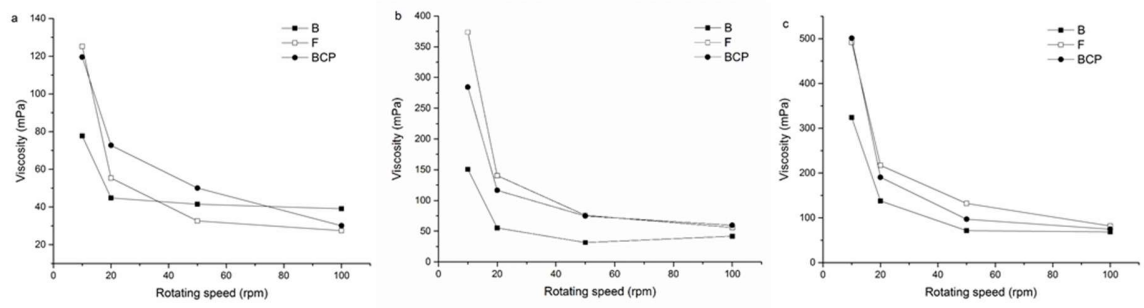

239 **Figure 4.** Rotational viscosities of DES-treated and microfluidized pulps after passing
240 through the a) 400 µm and 200 µm chambers, b) 400 µm and 100 µm chambers, and c) 400
241 µm and 87 µm chambers at a consistency of 0.3%.

The stereomicroscopic images of the DES-treated pulps after the third pass through the Masuko grinder are shown in supplemental material in Figure S1. The images show that the DES-treated pulps were already externally fibrillated at the beginning of the grinding process, while the NaOH-swollen fibers remained virtually untouched. Thus, the DES treatment clearly loosened the structure of the cellulose cell wall so that the fibrils began unraveling from the surface of the cellulose fibers. Previously, Abbott et al. (2006) used choline chloride-urea DES in the cationic functionalization of cotton cellulose. After a 15-hour reaction at 90˚C with sodium hydroxide, they had a cationic substitution of 0.22%, which increased the hydrophilicity of the cellulose material and its water absorption capacity by 26 wt.%. In our experiments, the reaction time was notably shorter (two hours) without sodium hydroxide, but highly swollen fibers were clearly observed after the addition of water at the end of the reaction, even without functionalization. The NaOH treatment also caused the fibers to swell, but not to the same extent as the DES treatment.

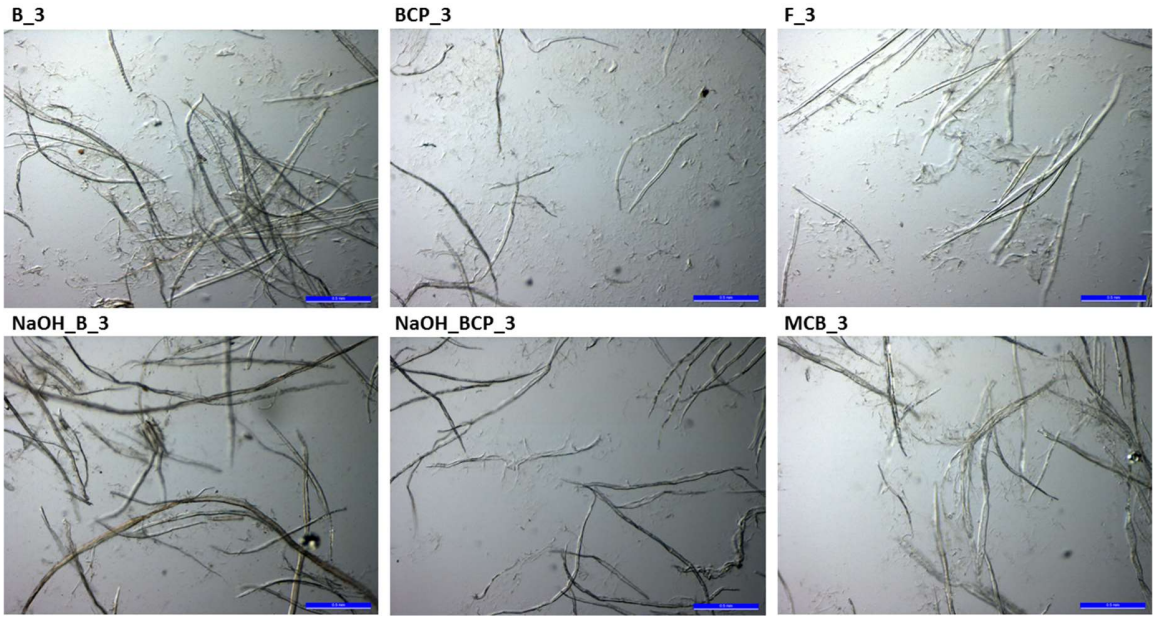

Figure S1. Optical microscopic images of pulps after the DES (B, BCP, F, and MCP) or NaOH treatment and the third pass through the Masuko grinder (scale bar 0.5 mm).

X-ray diffractometry

Figure 5 shows the crystallinities of the DES/NaOH-treated and Masuko-ground pulps and the crystallinities of the microfluidizer-treated pulps. The WAXD diffractograms (Figure 5a and b) indicate that the chemical and mechanical treatments left the cellulose I crystalline structure intact, with no rearrangement of the cellulose structure into other crystalline forms nor any notable dissolution of the cellulose occurring (French, 2014). Moreover, it appears that the DES treatment did not dissolve the crystalline parts of the cellulose. Similar observations have been made previously when using wood cellulose (Sirviö et al., 2015), and in reactions with chitin (Sharma et al., 2013). The Masuko grinding decreased the crystallinity of the NaOH-treated BCP linearly through nanofibrillation, while the crystallinity of the other pulps was slower during the first five passes (Figure 5c). After increasing the severity of the grinding (> 5 passes), the crystallinity index also significantly decreased for all of the DES-treated pulps.

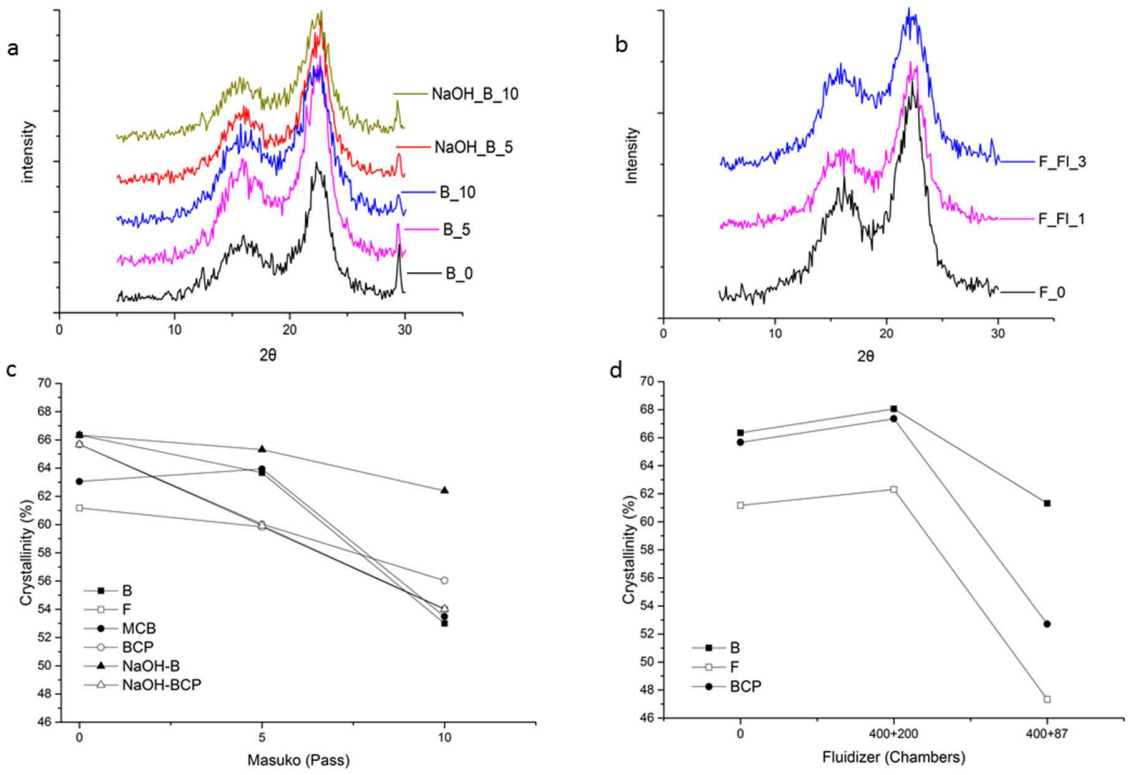

Figure 5. Examples of the diffractograms of the a) Masuko-ground B pulps and b)

273 microfluidizer-treated F pulps, and the crystallinity of the c) Masuko-ground samples and
274 the d) microfluidizer-treated samples.

275 The crystallinity of the samples increased at the beginning of the nanofibrillation with the
276 microfluidizer (Figure 5d), which was likely a consequence of the dissolving
277 hemicelluloses due to the high-pressure conditions of microfluidization. In addition, the
278 high shearing action during the homogenization process may have resulted in damage,
279 either through a breaking effect or the peeling-off of the cellulose chains on the surface of
280 the crystallite (Besbes et al., 2011). The decrease in the crystallinity of the pulp at the end
281 of the Masuko grinder treatment was highest for the B (20%) and lowest for the NaOH-
282 treated B (6%), but with the microfluidizer, the decrease in the crystallinity was highest for
283 the F (22%) and lowest for the B (7%) samples. Mechanical shearing causes a reduction in
284 the crystallinity of the cellulose fibers, but the level of damage to the crystalline parts is
285 highly affected by the refining mechanisms and chemical pretreatments and conditions
286 (Besbes et al., 2011; Ouajai & Shanks, 2006). The DES treatment and nanofibrillation with
287 the Masuko grinder clearly had the most efficient impact on the board pulp. However, there
288 were no significant differences between the nanofibrillation methods with the other pulps.
289 The crystallinity index of the nanofibrillated and DES-pretreated samples varied from 61%
290 to 47%.

291 *Visualization*

292 The FESEM images of the samples after the fifth pass through the Masuko grinder (Figure
293 6) showed the highly nanofibrillated form of the DES-treated BCP sample, but only a low
294 degree of nanofibrillation was achieved with the NaOH-treated pulp. The DES-treated B
295 and MCB samples also included larger residual particles, indicating only partial
296 disintegration of these board fibers. In addition, the FESEM images indicated that the F

297 pulp and BCP were more easily nanofibrillated during the microfluidizer treatment than the
298 B pulp. After passing through the largest chambers, the DES-treated BCP and F samples
299 consisted of fine nanofibrils, while the B sample had larger bunches of nanofibrils.
300 However, both the B and F pulps contained high quantities of lignin, and all three pulps had
301 notable amounts of hemicellulose (Figure 1), so the chemical composition may not explain
302 the differences in the degree of nanofibrillation. However, the ash content is highest in the
303 B pulp, which is caused by large quantities of fillers (Figure 1).

304 High filler content may affect the refining process in used two types of fibrillation
305 equipment. In the Masuko grinder, the fiber suspension is fed between two grinding disc
306 surfaces, one of which is stationary and the other rotary. The gap between the grinder discs
307 and the fitted bars and grooves on the discs' surface can be adjusted. By controlling these
308 parameters, it is possible to tune the intensity and flow patterns of the grinder (Dufresne,
309 2012; Spence, Venditti, Rojas, Habibi, & Pawlak, 2011). The fibers are fed to the hopper
310 and dispersed by centrifugal force; the fibers are designed to accommodate shear stress in
311 their longitudinal direction. The grinder causes internal and external fibrillation of the
312 fibers as well as the cutting of fibers when they are exposed to strong compression, rolling,
313 and shear forces (Abdul Khalil et al., 2014; Dufresne, 2012). The external fibrillation
314 modifies the fibers' surface layer by unraveling individual fibrils from the fibers' surface.
315 The inner fibrillation breaks down the fibers' internal bonding and thereby loosens the fiber
316 cell wall structure, which eases the separation of individual fibrils (Iwamoto, Nakagaito, &
317 Yano, 2007; Nakagaito & Yano, 2004). Filler particles do not cause any problems in this
318 kind of fibrillation system; on the contrary, they might even improve fibrillation by
319 grinding fibers between the grinding discs.

320 With the microfluidizer, the fiber suspension is fed to the inlet reservoir where the
321 intensifier pump supports the suspension with a constant flow and near constant pressure.

The fiber suspension is pumped through narrowing interaction chambers with velocities up to 500 m/s and pressure up to 2724 bar (Microfluidics Corporation, 2017). In the interaction chambers, fibers collide with each other and with the wear-resistant surfaces of the chambers, which causes high-impact, high-shear, and cutting force. In the cross-point of the interaction chamber pipes, the streams are allowed to collide to inflict additional force upon the fibers (Dufresne, 2012; Microfluidics Corporation, 2017; Spence et al., 2011). The forces' impact and the high-pressure drop cause the fibrils to unravel from the fiber cell wall. In this kind of fibrillation method, the high filler content creates blocks within the interaction chambers; those particles do not necessarily improve the fibrillation of the fibers, and they might be abrasive for the passage of interaction chambers.

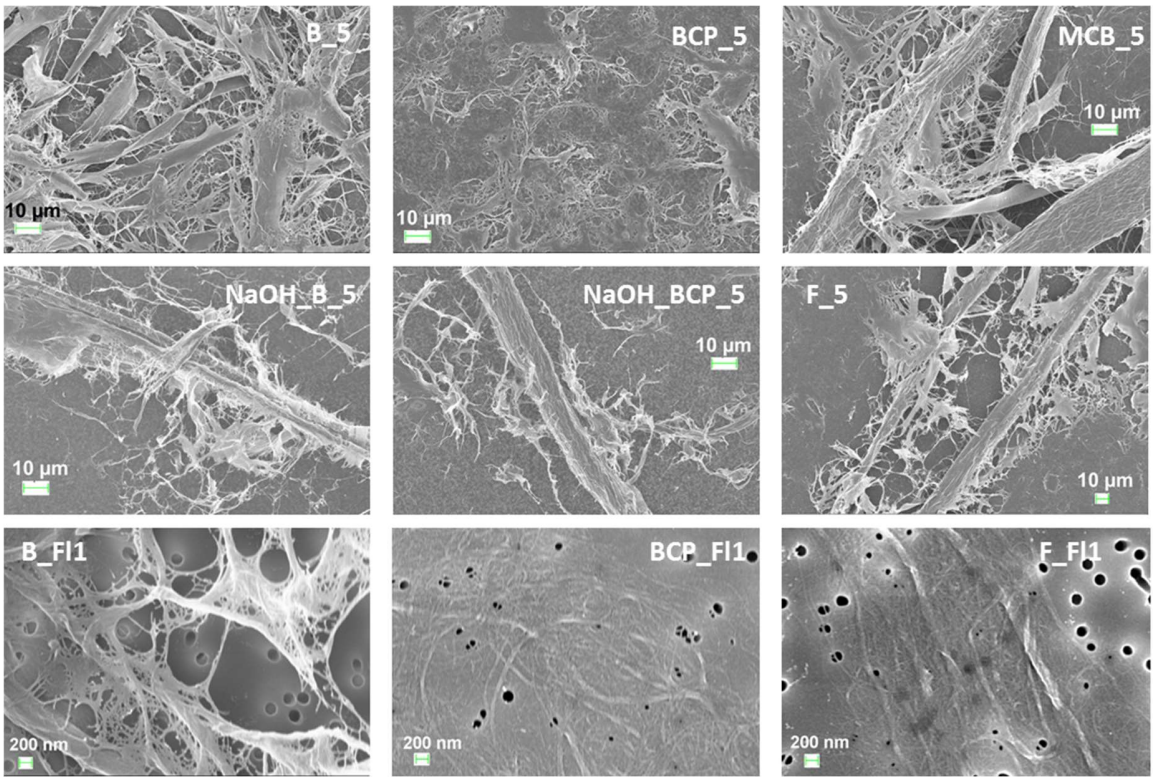

Figure 6. FESEM images of the DES/ and NaOH-treated pulps after the fifth pass through the Masuko grinder (top and middle rows) (scale bar 10 µm) and after passing through the 400 µm and 200 µm chambers of the microfluidizer (bottom row) (scale bar 200 nm).

Figure 7 shows the TEM images of the DES/NaOH-treated BCP and B pulp at the end of the Masuko grinding and microfluidization. Large bunches of nanofibrils (width from 15 nm to several hundred nm) are clearly visible in the NaOH-treated samples (Figure 7, middle). The visual appearances of the Masuko-ground (Figure 7, left) and microfluidized (Figure 7, right) DES-treated nanofibrils differ only slightly (width from 2 nm to 80 nm). The microfluidizer, where shear forces are high and long lasting for all fibers in the pulp, is one of the most effective machines to nanofibrillate cellulose fibers (Microfluidics Corporation, 2017). With the Masuko refiner, not all of the pulp's fibers are evenly exposed to shearing forces. Thus, it was likely that the Masuko-ground samples had slightly more bunches of nanofibrils than the microfluidization samples, but both nanofibrillation methods performed efficiently with all of the DES-treated pulps.

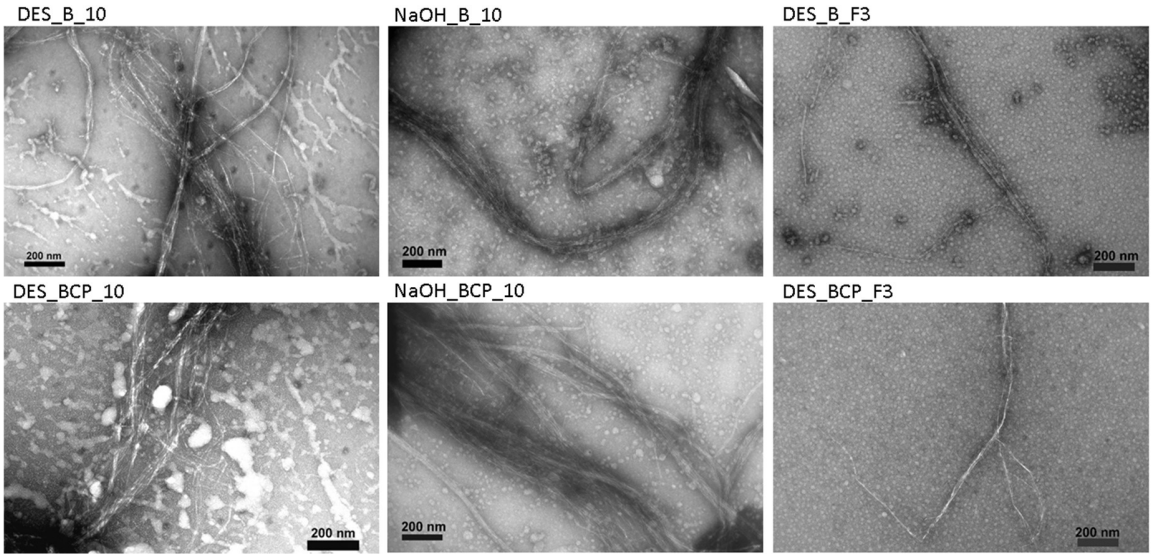

Figure 7. TEM images of the B and BCP samples (from left: Masuko 10th pass, NaOH-treated Masuko 10th pass, and microfluidizer 400 µm and 87 µm). The white dots in the images are from the poly-lysine in the sample preparation.

Mechanical handsheet properties

352 The properties of prepared board handsheets are shown in Table 1. Increase of mechanical
353 properties in paper with the addition of nanofibrillated cellulose is connected to the
354 increased bonding between cellulose fibers and cellulose nanofibrils. Increased bonding
355 between cellulose fibers and nanofibrils leads to increased stiffness and density (Delgado-
356 Aguilar et al., 2015; Hietala, Ämmälä, Silvennoinen, & Liimatainen, 2015a; Missoum,
357 Martoïa, Belgacem, & Bras, 2013; Taipale, Österberg, Nykänen, Ruokolainen, & Laine,
358 2010). Highest density and lowest bulk was observed in the board sheet with
359 microfluidizer-fibrillated BCP and Masuko-ground BCP, which also supports the previous
360 results of the most fibrillated material. Increased tensile strength of the board sheets with
361 the addition of different types of nanocellulose varied from 12.6% (NaOH-B) to 34.3% (B).
362 DES-treated and Masuko-ground board enhanced the tensile strength of the board sheets to
363 a greater extent than most fibrillated microfluidizer-treated BCP. Interactions between
364 fibers and nanocellulose fibrils not only increased the strength properties of the sheet but
365 also affected the formation of the sheet and the distribution of nanocellulose in the
366 handsheet (Hietala, Ämmälä, Silvennoinen, & Liimatainen, 2015b). Hietala, Ämmälä,
367 Silvennoinen, & Liimatainen (2015) and Ämmälä, Liimatainen, Burmeister & Niinimäki
368 (2013) noticed that the right dosage of nanocellulose as a strength enhancer is important, as
369 overdosing causes flocs—and, consequently, weaker formation and decreased strength
370 (Ämmälä, Liimatainen, Burmeister, & Niinimäki, 2013; Hietala et al., 2015b). Therefore,
371 the best doses of different types of nanocellulose might vary according to their chemical
372 composition, charge, and fibrillation stage. It is also possible that the best strength enhancer
373 is not the most fibrillated material, and those materials with long bunches of fibrils (such as
374 MCB) might work better. However, handsheet properties showed that Masuko grinding is a
375 more suitable fibrillation method for secondary fiber raw material sources. Increased board
376 handsheet properties also showed that DES-treated and Masuko-ground waste board and

paper nanocellulose are potential strength enhancers for the board, as all of the nanocellulose types this study used improved handsheet properties.

Table 1. The board handsheet properties (retention aid 0.08%, starch 4%, and nanocellulose 4%).

Sample	Grammage [g/m^2]	Density [kg/m^3]	Bulk [cm^3/g]	Tensile strength [kNm/kg]
0	152.8	695.1	1.53	33.39
BCP	158.1	711.6	1.35	42.32
F	153.2	686.2	1.46	41.49
B	152.9	710.0	1.41	44.84
MCB	157.7	699.7	1.43	42.97
NaOH_BCP	158.6	715.8	1.40	41.95
NaOH_B	159.0	702.1	1.42	37.59
BCP_F3	159.6	751.0	1.33	44.27
F_F3	163.0	717.5	1.39	38.43
B_F3	157.3	708.1	1.41	38.33

4. Conclusion

The choline chloride-urea DES pretreatment notably enhanced the nanofibrillation of the cellulose board pulp grades. Overall, the Masuko-ground and DES-treated samples had slightly larger nanofibril bunches than the microfluidization samples, but both nanofibrillation methods performed efficiently in all of the DES-treated pulps, resulting in long, fine individual nanofibrils and some nanofibril bunches. The nanofibril suspensions obtained from the DES pretreatment had viscous, gel-like appearances with shear thinning behavior. Moreover, the nanofibrils maintained their initial crystalline structure and had a crystallinity index of 61% to 47%. The additives and fillers in the waste board pulp diminished the degree of nanofibrillation in the microfluidizer, but in the Masuko grinder, all of the DES-treated board pulps were efficiently nanofibrillated. However, the DES-treated fluting pulp was nanofibrillated even better than the reference DES-treated bleached chemical pulp, resulting in the longest and finest nanofibrils. Overall, the largest nanofibril bunches were observed in the NaOH-swollen pulps (reference), indicating the lowest

degree of nanofibrillation. Properties of prepared board handsheets showed that Masuko grinding is a more suitable fibrillation method for secondary fiber raw material sources. Improved board handsheet properties also showed that DES-treated and Masuko-ground waste board and paper nanocellulose are potential strength enhancers for the board. Consequently, the DES chemical pretreatment appears to be a promising route to obtaining cellulose nanofibrils from waste board and paper.

Acknowledgments

The authors would like to acknowledge the funding provided by the Council of Oulu Region, granted by the European Regional Development Fund of the European Union for the High Performance Pretreatment of Lignocellulosic Biomasses for the Sustainable Biorefinery Value Chains Project (PREBIO).

References

Abbott, A. P., Bell, T. J., Handa, S., & Stoddart, B. (2006). Cationic functionalisation of cellulose using a choline based ionic liquid analogue. *Green Chemistry*, *8*(9), 784. https://doi.org/10.1039/b605258d

Abbott, A. P., Boothby, D., Capper, G., Davies, D. L., & Rasheed, R. K. (2004). Deep Eutectic Solvents Formed between Choline Chloride and Carboxylic Acids: Versatile Alternatives to Ionic Liquids. *Journal of the American Chemical Society*, *126*(29), 9142–9147. https://doi.org/10.1021/ja048266j

Abbott, A. P., Capper, G., Davies, D. L., Rasheed, R. K., & Tambyrajah, V. (2003). Novel solvent properties of choline chloride/urea mixturesElectronic supplementary information (ESI) available: spectroscopic data. See http://www.rsc.org/suppdata/cc/b2/b210714g/. *Chemical Communications*, (1), 70–71. https://doi.org/10.1039/b210714g

Abdul Khalil, H. P. S., Davoudpour, Y., Islam, M. N., Mustapha, A., Sudesh, K., Dungani, R., & Jawaid, M. (2014). Production and modification of nanofibrillated cellulose using various mechanical processes: A review. *Carbohydrate Polymers*, *99*, 649–665. https://doi.org/10.1016/j.carbpol.2013.08.069

Ämmälä, A., Liimatainen, H., Burmeister, C., & Niinimäki, J. (2013). Effect of tempo and periodate-chlorite oxidized nanofibrils on ground calcium carbonate flocculation and retention in sheet forming and on the physical properties of sheets. *Cellulose*, *20*(5), 2451–2460. https://doi.org/10.1007/s10570-013-0012-6

Ankerfors, M. (2012). *Microfibrillated cellulose energy-efficient preparation techniques and key properties*. Stockholm: Chemical Science and Engineering, KTH Royal Institute of Technology. Retrieved from http://urn.kb.se/resolve?urn=urn:nbn:se:kth:diva-102949 urn:nbn:se:kth:diva-102949

Azizi Samir, M. A. S., Alloin, F., & Dufresne, A. (2005a). Review of Recent Research into Cellulosic Whiskers, Their Properties and Their Application in Nanocomposite Field. *Biomacromolecules*, *6*(2), 612–626. https://doi.org/10.1021/bm0493685

Azizi Samir, M. A. S., Alloin, F., & Dufresne, A. (2005b). Review of Recent Research into Cellulosic Whiskers, Their Properties and Their Application in Nanocomposite Field. *Biomacromolecules*, *6*(2), 612–626. https://doi.org/10.1021/bm0493685

Besbes, I., Alila, S., & Boufi, S. (2011). Nanofibrillated cellulose from TEMPO-oxidized eucalyptus fibres: Effect of the carboxyl content. *Carbohydrate Polymers*, *84*(3), 975–983. https://doi.org/10.1016/j.carbpol.2010.12.052

Dai, Y., van Spronsen, J., Witkamp, G.-J., Verpoorte, R., & Choi, Y. H. (2013). Natural deep eutectic solvents as new potential media for green technology. *Analytica Chimica Acta*, *766*, 61–68. https://doi.org/10.1016/j.aca.2012.12.019

Danial, W. H., Abdul Majid, Z., Mohd Muhid, M. N., Triwahyono, S., Bakar, M. B., & Ramli, Z. (2015). The reuse of wastepaper for the extraction of cellulose nanocrystals.

446 *Carbohydrate Polymers*, *118*, 165–169.
447 https://doi.org/10.1016/j.carbpol.2014.10.072
448 Delgado-Aguilar, M., González, I., Pèlach, M. A., De La Fuente, E., Negro, C., & Mutjé, P.
449 (2015). Improvement of deinked old newspaper/old magazine pulp suspensions by
450 means of nanofibrillated cellulose addition. *Cellulose*, *22*(1), 789–802.
451 https://doi.org/10.1007/s10570-014-0473-2
452 Du, C., Zhao, B., Chen, X.-B., Birbilis, N., & Yang, H. (2016). Effect of water presence on
453 choline chloride-2urea ionic liquid and coating platings from the hydrated ionic
454 liquid. *Scientific Reports*, *6*, 29225. https://doi.org/10.1038/srep29225
455 Dufresne, A. (2012). *Nanocellulose: from nature to high performance tailored materials*.
456 Berlin ; Boston: De Gruyter.
457 Francisco, M., van den Bruinhorst, A., & Kroon, M. C. (2012). New natural and renewable
458 low transition temperature mixtures (LTTMs): screening as solvents for
459 lignocellulosic biomass processing. *Green Chemistry*, *14*(8), 2153.
460 https://doi.org/10.1039/c2gc35660k
461 French, A. D. (2014). Idealized powder diffraction patterns for cellulose polymorphs.
462 *Cellulose*, *21*(2), 885–896. https://doi.org/10.1007/s10570-013-0030-4
463 Hietala, M., Ämmälä, A., Silvennoinen, J., & Liimatainen, H. (2015a). Fluting medium
464 strengthened by periodate–chlorite oxidized nanofibrillated celluloses. *Cellulose*.
465 https://doi.org/10.1007/s10570-015-0801-1
466 Hietala, M., Ämmälä, A., Silvennoinen, J., & Liimatainen, H. (2015b). Fluting medium
467 strengthened by periodate–chlorite oxidized nanofibrillated celluloses. *Cellulose*.
468 https://doi.org/10.1007/s10570-015-0801-1
469 Iotti, M., Gregersen, Ø. W., Moe, S., & Lenes, M. (2011). Rheological Studies of
470 Microfibrillar Cellulose Water Dispersions. *Journal of Polymers and the*
471 *Environment*, *19*(1), 137–145. https://doi.org/10.1007/s10924-010-0248-2

Iwamoto, S., Nakagaito, A. N., & Yano, H. (2007). Nano-fibrillation of pulp fibers for the processing of transparent nanocomposites. *Applied Physics A*, *89*(2), 461–466. https://doi.org/10.1007/s00339-007-4175-6

Josset, S., Orsolini, P., Siqueira, G., Tejado, A., Tingaut, P., & Zimmermann, T. (2014). Energy consumption of the nanofibrillation of bleached pulp, wheat straw and recycled newspaper through a grinding process. *Nord Pulp Pap Res J*, *29*, 167–175.

Katz, S., Beatson, R. P., & Scallan, A. M. (1984). The determination of strong and weak acidic groups in sulfite pulps. *Svensk Papperstidning*, *65*(6), 48–53.

Kuutti, L., Pajari, H., Rovio, S., Kokkonen, J., & Nuopponen, M. (2016). Chemical recovery in TEMPO oxidation. *BioResources*, *11*(3), 6050–6061.

Lasseuguette, E., Roux, D., & Nishiyama, Y. (2008). Rheological properties of microfibrillar suspension of TEMPO-oxidized pulp. *Cellulose*, *15*(3), 425–433. https://doi.org/10.1007/s10570-007-9184-2

Lavoine, N., Desloges, I., Dufresne, A., & Bras, J. (2012). Microfibrillated cellulose – Its barrier properties and applications in cellulosic materials: A review. *Carbohydrate Polymers*, *90*(2), 735–764. https://doi.org/10.1016/j.carbpol.2012.05.026

Liimatainen, H., Sirviö, J., Pajari, H., Hormi, O., & Niinimäki, J. (2013). Regeneration and Recycling of Aqueous Periodate Solution in Dialdehyde Cellulose Production. *Journal of Wood Chemistry and Technology*, *33*(4), 258–266. https://doi.org/10.1080/02773813.2013.783076

Microfluidics Corporation. (2017). Microfluidics. web document. Retrieved from http://www.microfluidicscorp.com/

Missoum, K., Martoïa, F., Belgacem, M. N., & Bras, J. (2013). Effect of chemically modified nanofibrillated cellulose addition on the properties of fiber-based materials. *Industrial Crops and Products*, *48*, 98–105. https://doi.org/10.1016/j.indcrop.2013.04.013

Mohtaschemi, M., Sorvari, A., Puisto, A., Nuopponen, M., Seppälä, J., & Alava, M. J. (2014). The vane method and kinetic modeling: shear rheology of nanofibrillated cellulose suspensions. *Cellulose*, *21*(6), 3913–3925. https://doi.org/10.1007/s10570-014-0409-x

Nakagaito, A. N., & Yano, H. (2004). The effect of morphological changes from pulp fiber towards nano-scale fibrillated cellulose on the mechanical properties of high-strength plant fiber based composites. *Applied Physics A: Materials Science & Processing*, *78*(4), 547–552. https://doi.org/10.1007/s00339-003-2453-5

Ouajai, S., & Shanks, R. A. (2006). Solvent and enzyme induced recrystallization of mechanically degraded hemp cellulose. *Cellulose*, *13*(1), 31–44. https://doi.org/10.1007/s10570-005-9020-5

Paper Packaging Coordination Group (PPCG). (2016, May 20). The paper packaging industry's position and recommendations on the legislative proposals for amending Directive 94/62/EC on packaging and packaging waste (PPWD) and Directive 2008/98/EC on waste (WFD). Confederation of European Paper Industries, Position Paper. Retrieved from http://www.cepi.org/system/files/public/documents/positionpapers/recycling/2016/PPCG%20position_PPWD%20and%20WFD.pdf

Rattaz, A., Mishra, S. P., Chabot, B., & Daneault, C. (2011). Cellulose nanofibres by sonocatalysed-TEMPO-oxidation. *Cellulose*, *18*(3), 585–593. https://doi.org/10.1007/s10570-011-9529-8

Salam, A., Lucia, L. A., & Jameel, H. (2013). A Novel Cellulose Nanocrystals-Based Approach To Improve the Mechanical Properties of Recycled Paper. *ACS Sustainable Chemistry & Engineering*, *1*(12), 1584–1592. https://doi.org/10.1021/sc400226m

521 Segal, L., Creely, J. J., Martin, A. E., & Conrad, C. M. (1959). An empirical method for
522 estimating the degree of crystallinity of native cellulose using the X-ray
523 diffractometer. *Textile Research Journal*, *29*, 786–794.
524 Sharma, M., Mukesh, C., Mondal, D., & Prasad, K. (2013). Dissolution of α-chitin in deep
525 eutectic solvents. *RSC Advances*, *3*(39), 18149. https://doi.org/10.1039/c3ra43404d
526 Sirviö, J. A., Visanko, M., & Liimatainen, H. (2015). Deep eutectic solvent system based on
527 choline chloride-urea as a pre-treatment for nanofibrillation of wood cellulose. *Green*
528 *Chem.*, *17*(6), 3401–3406. https://doi.org/10.1039/C5GC00398A
529 Spence, K. L., Venditti, R. A., Rojas, O. J., Habibi, Y., & Pawlak, J. J. (2011). A comparative
530 study of energy consumption and physical properties of microfibrillated cellulose
531 produced by different processing methods. *Cellulose*, *18*(4), 1097–1111.
532 https://doi.org/10.1007/s10570-011-9533-z
533 Taipale, T., Österberg, M., Nykänen, A., Ruokolainen, J., & Laine, J. (2010). Effect of
534 microfibrillated cellulose and fines on the drainage of kraft pulp suspension and paper
535 strength. *Cellulose*, *17*(5), 1005–1020. https://doi.org/10.1007/s10570-010-9431-9
536 Zhang, Q., Benoit, M., De Oliveira Vigier, K., Barrault, J., & Jérôme, F. (2012). Green and
537 Inexpensive Choline-Derived Solvents for Cellulose Decrystallization. *Chemistry - A*
538 *European Journal*, *18*(4), 1043–1046. https://doi.org/10.1002/chem.201103271
539 Zhang, Q., De Oliveira Vigier, K., Royer, S., & Jérôme, F. (2012). Deep eutectic solvents:
540 syntheses, properties and applications. *Chemical Society Reviews*, *41*(21), 7108.
541 https://doi.org/10.1039/c2cs35178a
542 Zhang, S., Wang, W.-C., Li, F.-X., & Yu, J.-Y. (2013). Swelling and dissolution of cellulose
543 in NaOH aqueous solvent systems. *Cellulose Chem. Technol*, *47*, 671–679.
544
545